Eur. Phys. J. B **40**, 453–458 (2004)
DOI: 10.1140/epjb/e2004-00211-1

THE EUROPEAN PHYSICAL JOURNAL B

Effect of N isotopic mass on the photoluminescence and cathodoluminescence spectra of gallium nitride

F.J. Manjón[1,a], M.A. Hernández-Fenollosa[1], B. Marí[1], S.F. Li[2], C.D. Poweleit[2], A. Bell[2], J. Menéndez[2], and M. Cardona[3]

[1] Dpto. de Física Aplicada, Universitat Politècnica de València, 46071 Valencia, Spain
[2] Department. of Physics and Astronomy, Arizona State University, Tempe, AZ 85287, USA
[3] Max-Planck-Institut für Festkörperforschung, Heisenbergstr. 1, 70569 Stuttgart, Germany

Received 5 December 2004
Published online 20 July 2004 –

Abstract. GaN is a wurtzite-type semiconductor at ambient conditions whose natural composition consists of almost pure ^{14}N (99.63% ^{14}N and 0.37% ^{15}N) and a mixture of 60.1% ^{69}Ga, and 39.9% ^{71}Ga. We report a low-temperature photoluminescence and cathodoluminescence study of GaN thin films made from natural Ga and N, and from natural Ga and isotopically pure ^{15}N. The contribution of the nitrogen vibrations to the bandgap renormalization by electron-phonon interaction has been estimated from the nitrogen isotopic mass coefficient of the bound exciton energy. The temperature dependence of the bandgap of GaN can be explained with the measured isotopic mass coefficients of Ga and N. We have estimated the aluminum and indium contribution to the bandgap renormalization in AlN and InN from the temperature dependence of the AlN and InN bandgap up to 300 K, assuming that the N contribution is similar to that found in GaN. The similar bandgap isotopic mass coefficients of C, N, and O, of Al, Si and P, of Zn, Ga and Ge, and of Cd and In suggests that elements of the same row of the periodic table have similar bandgap isotopic mass coefficients.

PACS. 71.20.Nr Semiconductor compounds

1 Introduction

Nitride semiconductors are important materials for optoelectronic applications [1]. The most thoroughly studied member of this important family is GaN, which at ambient conditions is a wurtzite-type semiconductor with a fundamental bandgap near 3.42 eV. GaN thin films can be grown by various methods, including metal-organic chemical vapor deposition (MOCVD) and molecular beam epitaxy (MBE). Unintentionally doped GaN thin films grown by MBE are moderately n-type due to the presence of unbalanced donor and acceptor impurities [2].

It is well known that the bandgap energy of semiconductors depends on the average isotopic mass [3,4]. This dependence has been previously reported for GaN-related materials such as ZnO [5–8], but we are not aware of any similar report for GaN. In this paper we present a study of the low-temperature photoluminescence (PL) and cathodoluminescence (CL) of two unintentionally doped GaN thin films grown by MBE with natural Ga and different N isotopic compositions. Our main interest is the shift of the luminescence features as a function of the isotopic masses in order to obtain the isotopic contribution of nitrogen to the electron-phonon renormalization. The isotopic mass dependence of the luminescence can be used to model the well-known temperature dependence of the GaN bandgap [9,10].

2 Experimental procedure

Nominally-undoped isotopic GaN thin films were grown on c-axis oriented sapphire substrates by plasma-induced molecular beam epitaxy (PIMBE) using $^{14}N_2$ (99.6%) and highly enriched $^{15}N_2$ (99.5%) precursor gases. The two samples used in this study were prepared in the same manner, with the substrate temperature set at 800 °C and with a deposition rate of 0.5 μm/h without AlN buffer layer. The thicknesses of the layers are 1.0 and 1.3 microns for the $^{nat}Ga^{15}N$ and $^{nat}Ga^{14}N$ films, respectively [11]. The $^{nat}Ga^{15}N$ layer has a higher concentration of oxygen impurities because the $^{15}N_2$ precursor gas is only available in lower purity than $^{14}N_2$ [12]. Further details of the MBE growth are reported elsewhere [13].

Two different runs of low-temperature non-polarised PL measurements were performed with the samples in a backscattering geometry. For run A, the samples were placed inside a helium closed-cycle cryostat at 15 K and

[a] e-mail: fjmanjon@fis.upv.es

the PL was excited using the 325.2-nm line of a HeCd laser. The excitation power level was 30 mW. The emitted light was analyzed by a Jobin-Yvon HR460 spectrometer using a GaAs PMT detector optimized for the UV-VIS range. Calibration of PL lines was performed using the 388.865 nm line of He-I atom and the 441.563 nm line of Cd-II ion. For run B, the samples were placed in a similar cryostat at 12 K and the PL was also excited with the 325.2-nm line of a HeCd laser, but the power was reduced by a factor of 1,000 with respect to the prior measurement. The emitted light was analysed with a 0.5 m single-stage spectrometer (ACTON Research Corporation, Acton, MA) with a spectral resolution of 0.8 nm (0.7 meV) and detected with a CCD. The wavelength was calibrated with a Hg-lamp, and the CCD non-linearities were corrected in such a way that peak energies are reproducible within 0.01 nm, regardless of the peak pixel position on the CCD. Cathodoluminescence spectra were taken at 4 K using an electron beam energy of 5 keV and a beam current of 200 pA. The spectrometer resolution was set at 1.3 nm (1.4 meV).

3 Results and discussion

Figure 1 shows representative photoluminescence spectra at 15 K of the GaN samples under the conditions of run A. The PL spectra at 15 K are dominated in all samples measured by a band around 358 nm (3.459–3.461 eV for the natural sample). According to the literature, epitaxial GaN thin films grown on sapphire are under compressive planar stress which increases the energy values of the excitonic transitions and the separations between them [1]. In this sense, the band observed in our PL spectra can be attributed to the emission of a bound exciton in which a neutral acceptor is involved [1]. Figure 2 shows the detail of the PL spectra around the bound exciton emission. A clear blue shift of the peak energy of the bound exciton luminescence is observed in all spectra when the N isotopic mass is increased. Spectra obtained under the conditions of run B are similar in shape and show a similar isotopic mass dependence. Figure 3 shows low-temperature cathodoluminescence spectra. The spectral line shape as well as the nitrogen-mass dependence are consistent with the photoluminescence measurements.

Since we have measured only two samples of each isotopic composition, several measurements have been performed in different regions of the samples. For the present study, we have taken the average value of the energies found after several measurements as the nominal energy of the bound exciton for the definite isotopic composition. Figure 4 shows the dependence of the average peak energy of the bound exciton versus the nitrogen mass for the three types of measurements. In each case, the N-mass dependence of the bound exciton is fit with a straight line. The slope of those lines gives the isotopic mass coefficient corresponding to nitrogen. Notice that there are uniform shifts between the lines corresponding to the three types of measurement. These shifts are not significant, since they

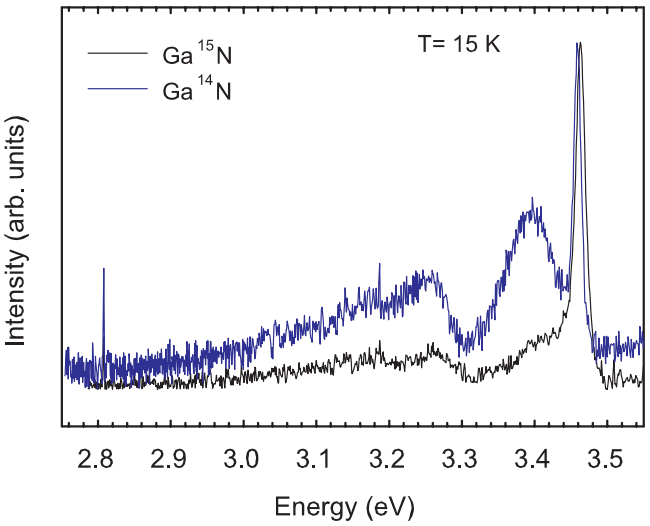

Fig. 1. Selected PL spectra of isotopically enriched GaN samples at 15 K. The intensities have been normalized at the maximum value which corresponds to the bound exciton.

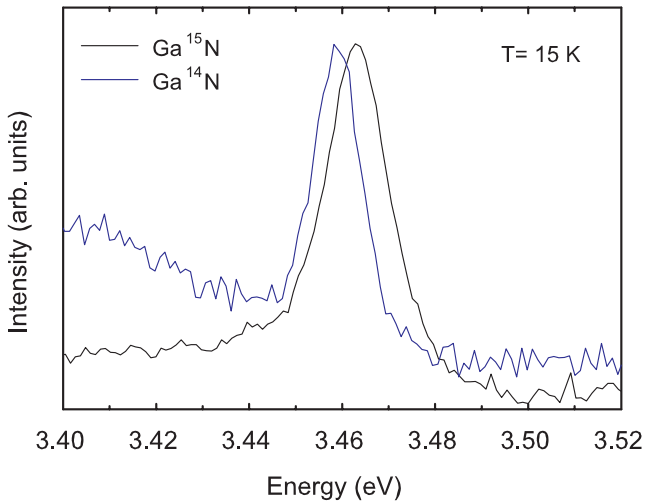

Fig. 2. Selected PL spectra of isotopically enriched GaN samples at 15 K in the bound exciton region. The intensities have been normalized at the maximum value, which corresponds to the bound exciton.

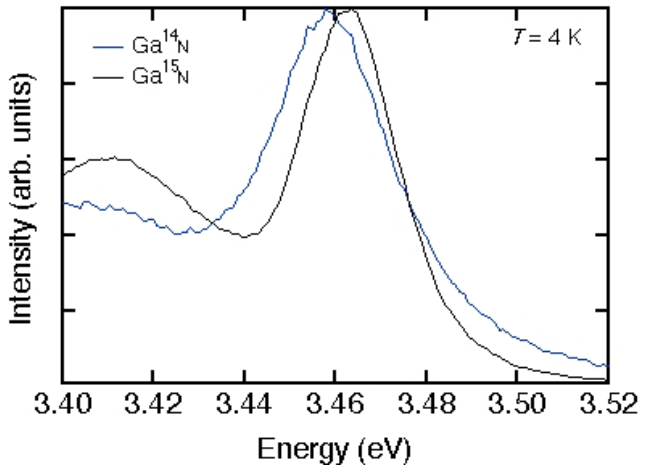

Fig. 3. Low-temperature CL spectra of isotopically enriched GaN samples. The intensities have been normalized at the maximum value, which corresponds to the bound exciton.

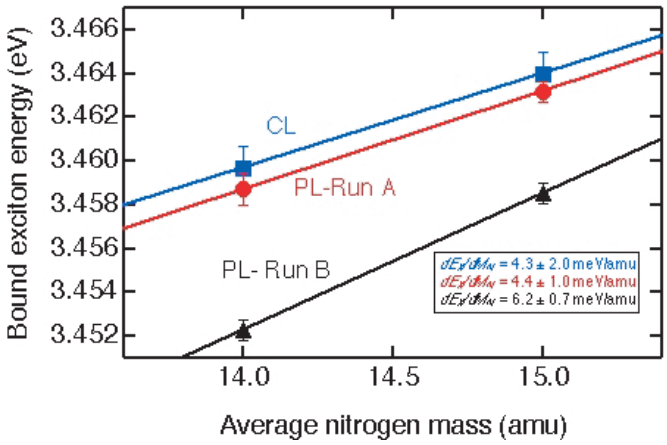

Fig. 4. Average bound exciton energies of the two measured isotopic samples of GaN at low temperatures. The lines represent linear fits to the nitrogen mass dependence of the bound exciton energy.

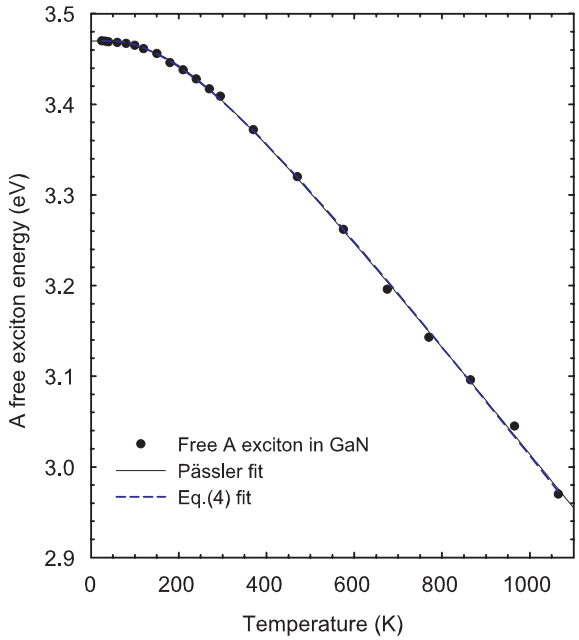

Fig. 5. Energy of the free A exciton in natural GaN samples as a function of temperature up to 1100 K (see Ref. [10]). The black solid line corresponds to a fit of the data to a two-oscillator model according to Pässler with equation (3). Blue dashed line corresponds to a fit of the data to a two-oscillator model, using equation (4).

are mainly due to small energy calibration differences between the three setups. Combining the three measurements, we arrive at a bandgap isotopic mass coefficient for N of $dE_x/dM_{\rm N} = 5.0 \pm 1.0$ meV/amu.

In order to discuss the PL and CL results, we assume that the observed renormalization of the bandgap ΔE_g due to isotopic substitution in both types of measurements is proportional to $M^{-1/2}$ [3]. The difference between the zero-point bandgap renormalization energies for two different isotopic compositions can then be described by the relation [3,8]

$$\Delta E_g(A) - \Delta E_g(B) = \Delta E_g \left(\frac{M(A) - M(B)}{M(A) + M(B)}\right) \qquad (1)$$

where ΔE_g(A) and ΔE_g(B) represent the zero-point gap renormalization for two isotopes A and B with masses M(A) and M(B), respectively. The energy difference of the average bound excitons for two different isotopes can be assumed to be equal to the l.h.s of equation (1), [4] and the knowledge of the isotopic masses of the two samples allows us to obtain the zero-point gap renormalization ΔE_g. Therefore, using the nitrogen isotopic mass coefficient (5.0 ± 1.0 meV/amu), we obtain a contribution of N to the zero-temperature renormalization energy, $\Delta E_g(N) = -2M_{\rm N} dE_X/dM_{\rm N} = -145 \pm 30$ meV. The total bandgap renormalization is given by the addition of the nitrogen and gallium contributions [8]:

$$E(0) = E_0 - 2M_{\rm Ga}\frac{dE}{dM_{\rm Ga}} - 2M_{\rm N}\frac{dE}{dM_{\rm N}}, \qquad (2)$$

where E_0 is the bare bandgap energy. Using $2M_{\rm N}(dE_X/dM_{\rm N}) = 145 \pm 30$ meV and the isotopic mass coefficient of Ga measured in GaAs (0.39 ± 0.06 meV/amu) [14], we obtain $2M_{\rm Ga}(dE_X/dM_{\rm Ga}) = -54 \pm 8$ meV, and $E_0 - E(0) = 199 \pm 38$ meV.

We now show that the temperature dependence of the GaN bandgap, shown in Figure 5 [15], is consistent with the bandgap renormalization obtained from the isotopic dependence of the luminescence energy. Our analysis is based on a model proposed by Pässler [16]. Within this model, the phonons that induce the bandgap renormalization via the electron-phonon interaction are described by two effective oscillators representing optic and acoustic phonons, respectively. This leads to an expression of the form:

$$E(T) = E_0 - \alpha \left[w_1\, \theta_1 \left(\frac{1}{\exp(\theta_1/T) - 1} + \frac{1}{2}\right) + (1 - w_1)\, \theta_2 \left(\frac{1}{\exp(\theta_2/T) - 1} + \frac{1}{2}\right)\right]. \qquad (3)$$

The adjustable parameters of the model are E_0, α an effective electron-phonon coupling factor; w_1, a weighting factor ($0 < w_1 < 1$) that determines the relative strength of the coupling to each of the two oscillators; θ_1, the average frequency of the acoustic phonons (in temperature units); and θ_2, the average frequency of the optic phonons. From a fit of the experimental temperature dependence of the bandgap, Pässler obtains $\alpha = 0.000614$ eV/K, $w_1 = 0.34$, $\theta_1 = 270$ K and $\theta_2 = 755$ K. Thus, $E_0 - E(0) = (\alpha w_1 \theta_1 + \alpha(1 - w_1)\theta_2)/2 = 181$ meV, in rather good agreement with the value $E_0 - E(0) = 199$ meV obtained above. The fit parameters θ_1 and θ_2 correspond to average phonon frequencies of 186 cm^{-1} (23 meV) and 521 cm^{-1} (65 meV). This is in good agreement with the known phonon density of states in GaN [17,18], which shows a peak near 20 meV and a large gap between 45 meV

and 65 meV separating the acoustic-like and optic-like branches.

We can further understand the temperature dependence of the bandgap in terms of its isotopic mass dependence if we associate the low-energy phonons with Ga-related motions and the high-energy phonons with N-related motions. Then, by equating the $T \to 0$ limit of equation (3) with equation (2), we obtain:

$$E(T) = E_0 - 2M_{\rm Ga}\frac{dE}{dM_{\rm Ga}}\left[\frac{2}{\exp\left(\theta_1/T\right)-1}+1\right] - 2M_{\rm N}\frac{dE}{dM_{\rm N}}\left[\frac{2}{\exp\left(\theta_2/T\right)-1}+1\right]. \quad (4)$$

Thus Pässler's fit of the temperature dependence of the bandgap implies $2M_{\rm Ga}(dE_X/dM_{\rm Ga}) = \alpha w_1\theta_2/2 =$ 28 meV and $2M_{\rm N}(dE_X/dM_{\rm N}) = [\alpha(1-w_1)\theta_2]/2 =$ 152 meV. This is in reasonable agreement with the actual isotopic measurements, especially for the largest contribution arising from the N-atoms.

Alternatively, we can fit the temperature dependence of the bandgap using equation (4) with the experimental isotopic mass dependence of the bandgap as an input and taking only the phonon frequencies as adjustable parameters. If we insert $dE/dM_{\rm N} = 5.0$ meV/amu and $dE/dM_{\rm Ga} = 0.39$ meV/amu, we obtain the excellent fit shown in Figure 5. From this fit we obtain $\theta_1 = 327$ K and $\theta_2 = 975$ K, indicating that the temperature dependence of the GaN bandgap is described by an average acoustic phonon of 174 cm^{-1} (21.6 meV) and an average optical phonon of 677 cm^{-1} (84 meV). These values are in even better agreement with the phonon density of states in GaN.

It has been suggested that the total bandgap renormalization can be obtained by extrapolation of a straight line from the high temperature region (around 1000 K) to $T = 0$ K. Using this procedure, we obtain $E_0 - E(0) =$ 138 meV, which is significantly less than the total bandgap energy renormalization of about 180–200 meV obtained above. This discrepancy indicates that linear extrapolations should be performed with extreme care. It is apparent from equations (3) and (4) that the linear regime corresponds to very small values of θ_1/T and θ_2/T, at least on the order of 0.1. In GaN, θ_2 is near 900 K, so that 1100 K cannot be considered as "high temperature". This explains why the extrapolated total bandgap energy renormalization for GaN (138 meV) underestimates the values 181 and 199 meV deduced from a fit of the temperature dependence using equations (3) and (4). It also suggests that many extrapolated total bandgap energy renormalizations at zero-temperature in other semiconductors underestimate the value of the total bandgap energy renormalization, since the range of temperatures taken for the extrapolation can not be considered as "high temperature".

The temperature dependence of the bandgap has been recently determined, up to 300 K, for AlN [19] and InN [20]. Since 300 K cannot be considered as "high temperature", as discussed above, it is not possible to obtain an accurate value of the total bandgap renormalization in these materials using a linear-extrapolation procedure. Instead, we fit the temperature dependence of the AlN and InN bandgaps using equation (4) with a single oscillator corresponding to the heaviest element (Al or In). The reason for using a single oscillator is that in the low temperature range measured (up to 300 K) the temperature dependence should correspond mainly to the activity of the acoustic modes (with the major contribution from the heaviest element). In order to do the fit with only one oscillator, we assume that the relative contribution of each phonon mode to the electron-phonon interaction is the same for the three nitrides. This means that the effective acoustic and optic phonon frequencies for AlN and InN can be obtained from those estimated for GaN (21.6 meV and 84 meV from the temperature fit) by identifying similar features in the corresponding phonon density of states. Using this approach, we find by inspection that the effective acoustic/optic phonon frequencies are 39/90 meV (AlN) and 12.5/72 meV (InN) [17]. Using equation (4) with one oscillator and fixing the effective acoustic phonon in AlN at 39 meV (450 K) and in InN at 12.5 meV (144 K) we find that the isotopic mass coefficient of Al is about 1.07 meV/amu, and that the isotopic mass coefficient of In is about 0.061 meV/amu. The fits are shown in Figures 6 and 7.

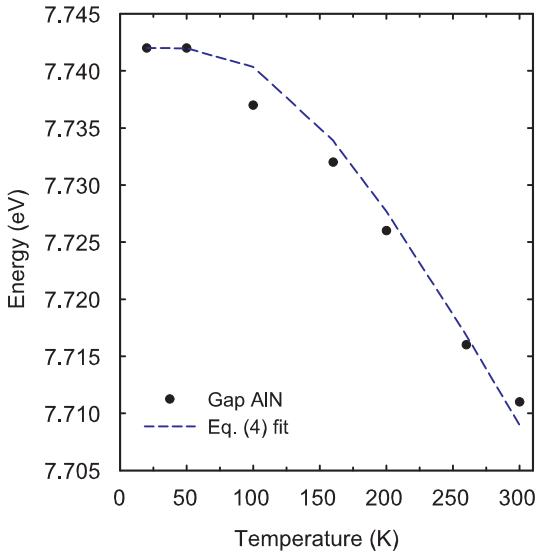

Fig. 6. Energy of the dominant feature of the reflectivity spectrum in natural AlN samples as a function of temperature up to 300 K (see Ref. [22]). Blue dashed line corresponds to a fit of the data to a one-oscillator model taking into account only acoustic vibrations, using equation (4).

Another possibility for estimating the isotopic mass coefficients for Al and In is to use the average frequencies of the acoustic branches. These are about 35 meV for AlN [21], and 18.6 meV for InN [17,22]. A fit of the temperature dependence of the AlN bandgap using an average phonon frequency of 35 meV gives an isotopic mass coefficient of 0.88 meV/amu. In the case of InN, the isotopic mass coefficient from the fit is 0.1 meV/amu.

Table 1. Elements and corresponding isotopic mass coefficients of the lowest gaps (in meV/amu).

	B	C (6.8) [4]	N (5.0)[a]	O (3.2) [8]
	Al (1.07) [a]	Si (0.5) [4]	P (0.95) [4]	S (0.74) [4]
Zn (0.42) [8]	Ga (0.39) [4]	Ge (0.18) [4]	As (0.34) [4]	Se (0.22) [4]
Cd (0.068) [4]	In (0.061)[a]	Sn	Sb	Te (0.1) [4]

[a] This work.

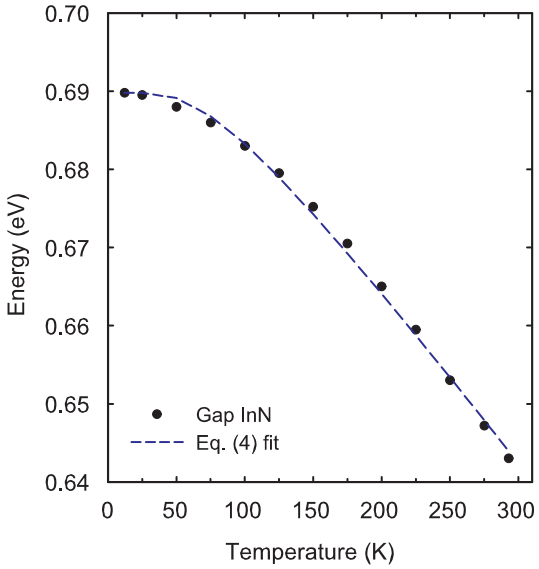

Fig. 7. Energy of the bandgap of InN as measured from the transmission spectrum as a function of temperature up to 300 K (see Ref. [23]). Blue dashed line corresponds to a fit of the data to a one-oscillator model taking into account only acoustic vibrations and using equation (4).

The estimated isotopic mass coefficients for Al (0.88–1.07 meV/amu) are close to the Si isotopic mass coefficient measured for the indirect gap in Si (0.53 meV/amu per each of the two primitive cell atoms) [23] and the P isotopic mass coefficient in GaP (0.95 meV/amu) [4]. Similarly, the estimated isotopic mass coefficients for In (0.061–0.1 meV/amu) are lower than that of Se (0.22 meV/amu) and on the same order of that found for Cd in CdS (40–60 μeV/amu) [24]. Furthermore, the estimated In isotopic mass coefficient suggests that the In contribution to the total bandgap energy renormalization in InN at zero temperature should be $\Delta E_g(\mathrm{In}) = -2 \cdot M_{\mathrm{In}} \cdot dE_x/dM_{\mathrm{In}} = -18$ meV; i.e., much smaller than the N contribution, which we assume to be the same (–145 meV) as in GaN.

The comparison between the isotopic mass coefficients of elements with similar masses can be further extended, since the measured isotopic mass coefficient of N (5 meV/amu) is midway between that of O (3.2 meV/amu) [8] and C (6.8 meV/amu per each of the two primitive cell atoms) [4]. Furthermore, the measured isotopic mass coefficient of Ga (0.39 meV/amu) [14] is similar to those found for Zn (0.42 meV/amu) [8] and Ge (0.18 meV/amu per each of the two primitive cell atoms) [25,26]. Therefore, our analysis suggests that elements of the same row of the periodic table exhibit similar bandgap isotopic mass coefficients, as shown in the Table 1. Therefore, similar contributions to the total bandgap energy renormalization at zero temperature are expected for the elements of the same row, as shown in Table 2. In other words, the fundamental bandgap renormalization is similar for compounds that contain elements of the same row. This conclusion explains the comparable bandgap renormalization energies found and discussed for ZnO and GaN [8].

Table 2. Elements and their estimated contributions to the total bandgap renormalization at zero temperature (in meV) according to the relation $\Delta \mathrm{E}_g(A) = -2M_A dE_x/dM_A$ and data from Table 1.

	B	C (170)	N (145)	O (109)
	Al (58)	Si (29)	P (59)	S (49)
Zn (55)	Ga (54)	Ge (26)	As (51)	Se (34)
Cd (15)	In (14)	Sn	Sb	Te (25)

4 Conclusions

In this work, we report a detailed study of the low-temperature photoluminescence and cathodoluminescence of two unintentionally doped GaN thin films with different nitrogen isotopic compositions. As a result, we have obtained the nitrogen isotopic mass coefficient from the isotopic shift of the bound exciton energy. The temperature dependence of the GaN bandgap up to 1100 K can be nicely fit with a two-oscillator model if we take the measured nitrogen (5.0 meV/amu) and gallium (0.39 meV/amu) isotopic coefficients. From the fit, the average acoustic and optic phonons contributing to the electron-phonon renormalization of the bandgap as a function of temperature are estimated. The gallium isotopic coefficient agrees nicely with those found previously for Zn and Ge. The study of the temperature dependence of AlN and InN according to the proposed equation (4) has allowed us to estimate the isotopic coefficients of Al and In. All measured and estimated bandgap isotopic coefficients are reviewed and a similar bangap isotopic coefficient for elements of the same row of the periodic table is found.

The incorporation of quasi-particle corrections to the energy bands obtained from density functional theory within the local density approximation has made it possible to predict energy gaps in semiconductors from first

principles. For the nitrides, the theoretical bandgaps are 3.5 eV (GaN, Ref. [27]), 5.8 eV (AlN, Ref. [27]) and 0.93 eV (InN, Ref. [28]). These values are usually compared with the experimental zero temperature bandgaps, 3.5 eV (GaN), 6.2 eV (AlN), and 0.69 eV (InN). However, the calculations assume that the ions are frozen in place, and therefore they should be compared with the bare bandgaps obtained by adding the zero-point renormalization to the experimental low-temperature value. In the case of the nitrides we find these values to be 200 meV (GaN and AlN) and 150 meV (InN). Thus the consideration of the bandgap renormalization worsens the agreement between theory and experiment for AlN and GaN, but improves it for InN.

The authors thank R. Lauck for a critical reading of the manuscript, R. Pässler for informative discussions, and M. Stutzmann for supplying the GaN samples. This work was supported through Spanish Government MCYT grant MAT2002-04539-C02-02 and Generalitat Valenciana OCYT grant GV01-211. F.J.M. acknowledges financial support by the "*Programa Incentivo a la Investigación de la U.P.V.*".A. Bell was supported by a grant from Nichia Corporation.

References

1. A.K. Viswanath, in *Handbook of Advanced Electronic and Photonic Materials and Devices*, Vol. 1, edited by H. Nalwa (Academic Press, San Diego, 2001), p. 109
2. N. Newman, in Gallium Nitride (GaN) I, *Semiconductors and Semimetals*, Vol. 50, edited by J.I. Pankove, T.D. Moustakas (Academic Press, San Diego, 1998), p. 84
3. M. Cardona, Phys. Stat. Solidi (b) **220**, 5 (2000)
4. T.A. Meyer, D. Karaiskaj, M.L.W. Thewalt, M. Cardona, Solid State Commun. **126**, 119 (2003)
5. D. Olguin, M. Cardona, A. Cantarero, Solid State Commun. **122**, 575 (2002)
6. F.I. Kreingol'd, Fiz. Tverd. Tela **27**, 3138 (1978) [Sov. Phys. Solid State **20**, 1810 (1978)]
7. F.I. Kreingol'd, B.S. Kulinkin, Fiz. Tverd. Tela **28**, 3164 (1986) [Sov. Phys. Solid State **27**, 1781 (1986)]
8. F.J. Manjón, M. Mollar, M.A. Hernández-Fenollosa, B. Marí, R. Lauck, M. Cardona, Solid State Commun. **128**, 35 (2003)
9. H. Teisseyre, P. Perlin, T. Suski, I. Grzegory, S. Porowski, J. Jun, A. Pietraszko, T.D. Moustakas, J. Appl. Phys. **76**, 2429 (1994)
10. H. Herr, Diplomarbeit, Technische Univeristät München, 1996
11. J.M. Zhang, T. Ruf, M. Cardona, O. Ambacher, M. Stutzmann, J.-M. Wagner, F. Bechstedt, Phys. Rev. B **56**, 14399 (1997)
12. M.W. Bayerl, N.M. Reinacher, H. Angerer, O. Ambacher, M.S. Brandt, M. Stutzmann, J. Appl. Phys. **88**, 3249 (2000)
13. H. Angerer, O. Ambacher, R. Dimitrov, Th. Metzger, W. Rieger, M. Stutzmann, MRS Internet J. Nitride Semicond. Res. **1**, 15 (1996)
14. N. Garro, A. Cantarero, M. Cardona, A. Göbel, T. Ruf, K. Eberl, Phys. Rev. B **54**, 4732 (1996)
15. R. Pässler, Phys. Rev. B **66**, 085201 (2002)
16. R. Pässler, J. Appl. Phys. **89**, 6235 (2001)
17. C. Bungaro, K. Rapcewicz, J. Bernholc, Phys. Rev. B **61**, 6720 (2000)
18. J.C. Nipko, C.-K. Loong, C.M. Balkas, R.F. Davis, Appl. Phys. Lett. **73**, 34 (1998); A. Debernardi, N.M. Pyka, A. Göbel, T. Ruf, R. Lauck, S. Kamp, M. Cardona, Solid State Commun. **103**, 297 (1997)
19. Q. Guo, M. Nishio, H. Ogawa, A. Yoshida, Solid State Commun. **126**, 601 (2003)
20. J. Wu, W. Walukiewicz, W. Shan, K.M. Yu, J.W. Ager III, S.X. Li, E.E. Haller, H. Lu, W.J. Schaff, J. Appl. Phys. **94**, 4457 (2003)
21. J.C. Nipko, C.-K. Loong, Phys. Rev. B **57**, 10550 (1998)
22. H.M. Tütüncü, G.P. Srivastava, S. Duman, Physica B **316-317**, 190 (2002)
23. D. Karaiskaj, M.L.W. Thewalt, T. Ruf, M. Cardona, M. Konuma, Solid State Commun. **123**, 87 (2002)
24. J.M. Zhang, T. Ruf, R. Lauck, M. Cardona, Phys. Rev. B **57**, 9716 (1998)
25. C. Parks, A.K. Ramdas, S. Rodríguez, K.M. Itoh, E.E. Haller, Phys. Rev. B **49**, 14244 (1999)
26. S. Zollner, M. Cardona, S. Gopalan, Phys. Rev. B **45**, 3376 (1992)
27. A. Rubio, J.L. Corkill, M.L. Cohen, E.L. Shirley, S.G. Louie, Phys. Rev. B **48**, 11810 (1993)
28. F. Bechstedt, J. Furthmüller, J. Crystal Growth **246**, 315 (2002)